WATER RESOURCES RESEARCH, VOL. 32, NO. 3, PAGES 583–593, MARCH 1996

Random-walk simulation of transport in heterogeneous porous media: Local mass-conservation problem and implementation methods

Eric M. LaBolle
Hydrologic Science, University of California, Davis

Graham E. Fogg
Hydrologic Science and Department of Geology, University of California, Davis

Andrew F. B. Tompson
Lawrence Livermore National Laboratory, Livermore, California

Abstract. The random-walk method for simulating solute transport in porous media is typically based on the assumption that the velocity and velocity-dependent dispersion tensor vary smoothly in space. However, in cases where sharp interfaces separate materials with contrasting hydraulic properties, these quantities may be discontinuous. Normally, velocities are interpolated to arbitrary particle locations when finite difference or finite element methods are used to solve the flow equation. The use of interpolation schemes that preserve discontinuities in velocity at material contacts can result in a random-walk model that does not locally conserve mass unless a correction is applied at these contacts. Test simulations of random-walk particle tracking with and without special treatment of material contacts demonstrate the problem. Techniques for resolving the problem, including interpolation schemes and a reflection principle, are reviewed and tested. Results from simulations of transport in porous media with discontinuities in the dispersion tensor show which methods satisfy continuity. Simulations of transport in two-dimensional heterogeneous porous media demonstrate the potentially significant effect of using a nonconservative model to compute spatial moments and breakthrough of a solute plume.

Introduction

The random-walk particle method (RWPM) has been used successfully for years to simulate conservative and reactive transport in porous media [*Ahlstrom et al.*, 1977; *Prickett et al.*, 1981; *Uffink*, 1985; *Tompson et al.*, 1987; *Tompson*, 1993]. This method is computationally appealing because it is grid independent and therefore, given the proper conditions, will require little computer storage relative to finite element, finite difference, and method of characteristic models. In addition, this method does not suffer from numerical dispersion in problems dominated by advection. Traditional finite element and finite difference models generally perform poorly under such conditions unless the computational grid is highly resolved. As a result, a random walk is often the method of choice for simulating transport in large, heterogeneous flow systems [*Tompson and Gelhar*, 1990; *Tompson*, 1993; *Tompson et al.*, 1994].

Global mass conservation is compulsory with the RWPM because particles cannot disappear. This distinct advantage of the RWPM, however, is often overstated; accurate solutions require local as well as global mass conservation.

In practice, the flow problem is often solved numerically, and velocities are interpolated to arbitrary particle locations. Advective particle tracking models can be made mass conservative by using a divergence-free velocity interpolation scheme [*Schafer-Perini and Wilson*, 1991]. However, additional criteria are necessary to formulate a mass conservative random-walk model. For example, discontinuities in the velocity or effective porosity may yield a dispersion tensor that is discontinuous in space. Local mass conservation conditions for the RWPM require that the dispersion tensor be continuous in space unless a reflection principle [*Feller*, 1957] or similar method is applied. Therefore, neglecting discontinuities in the dispersion tensor will result in local mass conservation errors. As these problems only occur when parameters are functions of the spatial coordinates, model errors will not necessarily be detected during routine verification checks.

In some applications of the RWPM to transport in heterogeneous porous media [e.g., *Tompson et al.*, 1987; *Tompson and Gelhar*, 1990], accuracy in local mass conservation has been traded for computational efficiency by specifying coefficients in the RWPM as block discrete (constant with a finite difference grid block). Though we do not believe this trade-off led to significant errors in the simulation results of *Tompson et al.* [1987] and *Tompson and Gelhar* [1990], results from random-walk simulations presented herein demonstrate that this approach violates local mass conservation and under certain circumstances can significantly affect solute-transport predictions. This paper reviews the conditions required for local mass conservation for the RWPM and demonstrates consequences

Copyright 1996 by the American Geophysical Union.

Paper number 95WR03528.
0043-1397/96/95WR-03528$05.00

of violating these conditions when the dispersion tensor is discontinuous due to a discontinuous velocity field. We discuss and demonstrate techniques for applying the RWPM in the presence of the discontinuities. Random-walk simulations of solute transport in two-dimensional heterogeneous porous media are presented that illustrate the potential effect of local mass conservation errors on simulation of a developing plume.

The Random-Walk Particle Method

The RWPM is commonly used in the field of statistical physics to model and analyze processes involving diffusion. In the hydrologic community, the approach has been widely applied to simulate advective and diffusive mass transport problems in subsurface systems [e.g., *Ahlstrom et al.*, 1977; *Prickett et al.*, 1981; *Uffink*, 1985; *Tompson et al.*, 1987]. Mass concentration of an aqueous solute is represented by a finite system of N_p particles of constant mass m_p via

$$\Theta c^p(\mathbf{x}, t) = \sum_{p \in N_p} m_p \delta[\mathbf{x} - \mathbf{X}_p(t)] \tag{1}$$

where Θ is the effective porosity, δ is a Dirac function, and $\mathbf{X}_p(t)$ is the location of particle p at time t. Because (1) is discontinuous, a modified expression of the form

$$\Theta c^s(\mathbf{x}, t) = \sum_{p \in N_p} m_p \zeta[\mathbf{x} - \mathbf{X}_p(t)] \tag{2}$$

is typically used to "smooth" the spatial distribution of concentration, where ζ is an interpolation, or projection function [*Bagtzoglou et al.*, 1992] normalized such that $\int_\Omega \zeta \, dV = 1$, where Ω is the domain of porous medium. The degree of smoothness obtained is controlled by the shape of ζ and the particle resolution N_r, the number of particles used to represent an arbitrary unit of mass. Mass in Ω is $M = \int_\Omega \Theta c \, dV = \Sigma_{p \in Np} m_p$.

Simulation of advective and diffusive mass transport may proceed by changing particle positions with time via an Itô-Taylor integration scheme, given as [*Gardiner*, 1990]

$$\mathbf{X}_p(t + \Delta t) - \mathbf{X}_p(t) = \mathbf{A}(\mathbf{X}_p, t)\Delta t + \mathbf{B}(\mathbf{X}_p, t) \cdot \Delta \mathbf{w}(\Delta t) \tag{3}$$

where $\mathbf{A}$ is a "drift" vector $[LT^{-1}]$, $\mathbf{B}$ is a tensor $[LT^{-1/2}]$ defining the strength of diffusion, and $\Delta \mathbf{w}$, a Wiener process $[T^{1/2}]$, is a vector of independent normally distributed random variables with zero mean and unit variance given as

$$\langle \Delta \mathbf{w} \rangle = \mathbf{0} \tag{4a}$$

$$\langle \Delta \mathbf{w} \Delta \mathbf{w} \rangle = \Delta t \mathbf{I} \tag{4b}$$

Here $\langle \ \rangle$ denotes the expected value, and $\mathbf{I}$ is the identity matrix.

The particle number density, $f \equiv (\Theta c^p / m_p)$, obtained through repeated use of (1) on all particles, satisfies the Itô-Fokker Planck equation [*Risken*, 1989]:

$$\frac{\partial f}{\partial t} + \nabla \cdot (\mathbf{A} f) - \frac{1}{2} \nabla\nabla : (\mathbf{B} \cdot \mathbf{B}^T f) = 0 \tag{5}$$

in the limit as $N_r \to \infty$ and $\Delta t \to 0$, where

$$\mathbf{A} = \lim_{\Delta t \to 0} \frac{1}{\Delta t} \langle [\mathbf{X}_p(t + \Delta t) - \mathbf{X}_p(t)] \rangle \tag{6}$$

$$\mathbf{B} \cdot \mathbf{B}^T = \lim_{\Delta t \to 0} \frac{1}{\Delta t} \langle [\mathbf{X}_p(t + \Delta t) - \mathbf{X}_p(t)]^2 \rangle \tag{7}$$

To simulate conservative transport, we wish to specify $\mathbf{A}$ and $\mathbf{B}$ in (5) such that the mass density satisfies the familiar advection-dispersion equation

$$\frac{\partial(\Theta c)}{\partial t} + \nabla \cdot (\mathbf{v}\Theta c) - \nabla \cdot (\Theta \mathbf{D} \cdot \nabla c) = 0 \tag{8}$$

In (8), c is the aqueous concentration $[ML^{-3}]$, $\mathbf{v}$ is the average groundwater velocity vector in the porous medium $[LT^{-1}]$, and $\mathbf{D}$ is the local hydrodynamic dispersion tensor $[L^2T^{-1}]$ [*Bear*, 1972],

$$\mathbf{D} = (\alpha_T |\mathbf{v}| + D^m)\mathbf{I} + \frac{\alpha_L - \alpha_T}{|\mathbf{v}|} \mathbf{v}\mathbf{v} \tag{9}$$

where $\alpha_L[L]$ and $\alpha_T[L]$ are the longitudinal and transverse dispersivities, respectively, and D^m is the molecular diffusivity of the porous medium $[L^2T^{-1}]$. By choosing $\mathbf{A}$ and $\mathbf{B}$ as [*Kinzelbach*, 1988; *Uffink*, 1988; *Tompson et al.*, 1987]

$$\mathbf{A} = \mathbf{v} + \nabla \cdot \mathbf{D} + \frac{1}{\Theta} \mathbf{D} \cdot \nabla\Theta \tag{10}$$

$$2\mathbf{D} = \mathbf{B} \cdot \mathbf{B}^T, \tag{11}$$

and noting that $m_p f = \Theta c^p$, (5) and (8) become equivalent. Substituting (10) and (11) into (3) yields the equation for a particle displacement

$$\mathbf{X}_p(t + \Delta t) - \mathbf{X}_p(t) = \left(\mathbf{v} + \nabla \cdot \mathbf{D} + \frac{1}{\Theta} \mathbf{D} \cdot \nabla\Theta \right) \Delta t + \mathbf{B} \cdot \Delta \mathbf{w} \tag{12}$$

where coefficients in the right-hand side of (12) are evaluated at $\mathbf{X}_p(t)$. Because $\mathbf{D}$ is real and symmetric, elements of the tensor $\mathbf{B}$ can be calculated by diagonalizing $\mathbf{D}$, taking the positive root of the eigenvalues, transforming back, and multiplying by an arbitrary orthogonal matrix $\mathbf{R}$ [*Risken*, 1989] (for details refer to *Tompson et al.* [1987]). In the case $|\mathbf{v}| = 0$ (stagnation point with a scalar diffusion function), we use $B_{ij} = (2D_m)^{1/2}$ for $(i = j)$ and $B_{ij} = 0$ for $(i \neq j)$. This development can be extended to treat reactive transport for constituents that undergo binary reversible equilibrium sorption [*Tompson*, 1993] and kinetic decay [*Tompson and Dougherty*, 1992].

Gradient Terms and Discontinuities in D

In some previous applications of the RWPM, the gradient terms in (12) have been ignored or overlooked [e.g., *Ahlstrom et al.*, 1977; *Prickett et al.*, 1981], leaving simply $\mathbf{A} = \mathbf{v}$. When $\mathbf{D}$ or Θ vary spatially, however, these gradients can be quite significant, as illustrated by applying the RWPM to find a steady state solution to the purely diffusive system with $\Theta = 1$,

$$\frac{\partial c}{\partial t} - \frac{\partial}{\partial x} D(x) \frac{\partial c}{\partial x} = 0 \tag{13}$$

for $0 < x < 1$, where $D(x) = 1 + 99x$, $c(0, t) = 1$, and $c(1, t) = 0$. Figure 1 shows the steady state analytical solution of this system [*Crank*, 1975] along with two coarse (i.e., noisy) particle solutions obtained from (12) with and without the gradient correction quantity in the drift term. Both particle solutions

were evolved over time to an approximate steady state at $t = 0.1$, based upon a zero initial condition, and properly maintained boundary conditions [*Tompson and Dougherty*, 1992]. Importance of the correction in the drift term (**A**) is clearly evident.

Because of their dependence on gradients of velocity, porosity, and dispersivity, the importance of the correction terms in hydrologic applications will be most significant near sharp wetting fronts, stagnation zones, material contacts, and abrupt changes in the flow field [*Uffink*, 1988; *Tompson et al.*, 1987]. General incorporation of gradient terms may require careful interpolation of velocities, porosities, dispersivities, and diffusivities. A problem arises, however, at contacts between materials with contrasting hydraulic properties. Here, effective porosities, dispersivities, diffusivities, and flow velocities, and therefore the velocity dependent dispersion tensor, may be discontinuous in space.

In the case of discontinuities in the dispersion tensor or effective porosity, the gradient terms in (12) are undefined. Ignoring the effect of discontinuities in the dispersion tensor will result in local mass conservation errors even in the limit as the time step approaches zero. In this paper we consider particle methods that address discontinuities in dispersion tensor caused by discontinuities in the velocity field only, and will consider dispersivities and porosity to be constant. Nevertheless, methods similar to those presented here can be applied to locally conserve mass where dispersivity and porosity have discontinuities.

In general, the statement expressing local mass conservation at an interface, denoted here by the surface **s**, is [*Gardiner*, 1990]

$$\lim_{x \to s} \mathbf{J}^- \cdot \mathbf{n} = \lim_{s \leftarrow x} \mathbf{J}^+ \cdot \mathbf{n} \tag{14}$$

$$\lim_{x \to s} c^- = \lim_{s \leftarrow x} c^+ \tag{15}$$

where **J** is mass flux, given as

$$\mathbf{J} = \Theta \mathbf{A} c - \Theta \mathbf{D} \cdot \nabla c \tag{16}$$

and **n** is the outward normal to **s**, and the superscript plus and minus refer to quantities on opposite sides of **s**. When **D** is discontinuous at $\mathbf{s} \in \Omega$, within the simulation domain, (14)

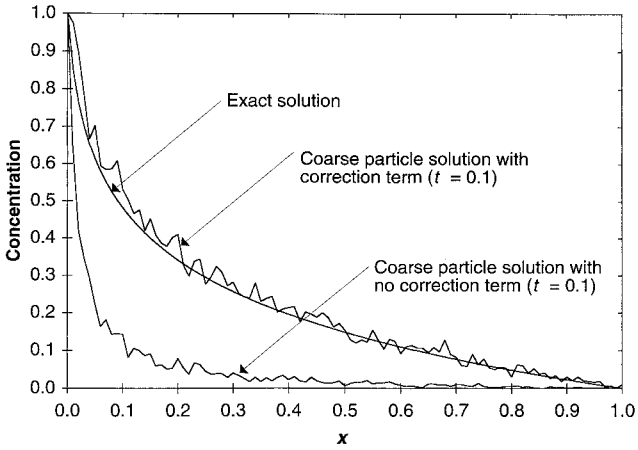

Figure 1. Analytical steady state solution to (13), compared with two, approximately steady state and coarse particle solutions at $t = 0.1$ obtained with and without gradient term.

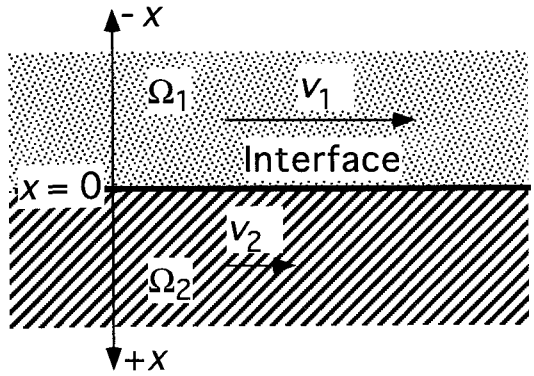

Figure 2. A two-layer system with a discontinuous diffusion coefficient across an interface.

may not be satisfied by the RWPM. Below, we review a reflection technique that has been developed to address this problem and introduce another approach based on interpolation of **D**.

Reflection and Interpolation Techniques

Uffink [1985] treated the problem of a discontinuous dispersion tensor through application of a reflection principle based on the method of images [*Feller*, 1957]. He applied this method to transport in stratified porous media with flow parallel to the bedding plane where the tangential velocity and velocity-dependent dispersion tensor are discontinuous at interfaces between strata (Figure 2). Here we present and test the method of *Uffink* [1985] and an alternative interpolation technique.

Reflection Principle

A reflection principle can be developed for one-dimensional diffusion across an interface with constant (yet different) diffusion coefficients on both sides of this interface and $\Theta = 1$ (Figure 2). Here we have

$$\frac{\partial c_1}{\partial t} = D_1 \frac{\partial^2 c_1}{\partial x^2} \qquad x < 0 \tag{17a}$$

$$\frac{\partial c_2}{\partial t} = D_2 \frac{\partial^2 c_2}{\partial x^2} \qquad x > 0 \tag{17b}$$

where D_1 and D_2 are the diffusion coefficients and the subscripts 1 and 2 refer to quantities in Ω_1 and Ω_2, respectively. Conservation of mass requires that

$$\lim_{x \to 0} D_1 \frac{\partial c_1}{\partial x} = \lim_{0 \leftarrow x} D_2 \frac{\partial c_2}{\partial x} \tag{18a}$$

$$\lim_{x \to 0} c_1 = \lim_{0 \leftarrow x} c_2 \tag{18b}$$

For the case of a partially reflecting interface, $D_1 > D_2 > 0$, an instantaneous point source in Ω_1, $c(x_0, 0) = 1$, $x_0 < 0$, and a system of infinite spatial extent, applying the method of images yields a solution to (17a) and (17b) in terms of source and reflected components (superscripts S and R, respectively) [*Carslaw and Jaeger*, 1959]:

$$c_1(x, t) = c_1^S(x, t) + c_1^R(x, t) \qquad x < 0 \tag{19a}$$

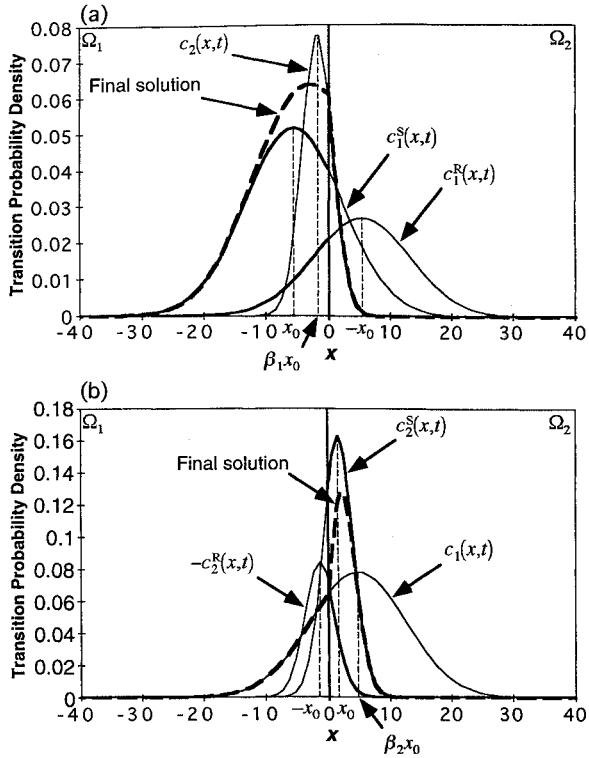

Figure 3. Component parts (bold lines) of analytical solution given in (a) equations (19a)–(19d) for point source in Ω_1 and (b) equivalent form of (19a)–(19d) for point source in Ω_2 are summed to form final solution (bold dashed line) about an interface.

$$c_1^S(x, t) = \frac{1}{(4\pi D_1 t)^{1/2}} \exp\left(\frac{(x - x_0)^2}{4D_1 t}\right) \tag{19b}$$

$$c_1^R(x, t) = \frac{R_1}{(4\pi D_1 t)^{1/2}} \exp\left(\frac{(x + x_0)^2}{4D_1 t}\right) \tag{19c}$$

$$c_2(x, t) = \frac{1 - R_1}{(4\pi D_2 t)^{1/2}} \exp\left(\frac{(x - x_0\beta_1)^2}{4D_2 t}\right) \qquad x > 0 \tag{19d}$$

where R_1 is a reflection coefficient and the factor $\beta_1 = (D_2)^{1/2}/(D_1)^{1/2}$ accounts for the difference in mean-square displacements between the two strata by effectively adjusting the origin of the source in $\Omega_1(x < 0)$ for solution in $\Omega_2(x > 0)$. In order to satisfy (18a) and (18b), $R_1 = [(D_1)^{1/2} - (D_2)^{1/2}]/[(D_1)^{1/2} + (D_2)^{1/2}]$. For a source located in $\Omega_2(x_0 > 0)$, replace R_1 with $R_2 = -R_1$ and β_1 with $\beta_2 = (D_1)^{1/2}/(D_2)^{1/2}$. This solution is illustrated in Figures 3a and 3b.

Development of a reflection principle based on the method of images for application to the RWPM in one dimension is easily accomplished by modifying the transition probability density (TPD) for $\mathbf{B} \cdot \Delta\mathbf{w}$ in (12), for a particle that may cross the interface in the following time step [*Uffink*, 1985]. The modification consists of summing the component parts of the modified density function given by (19a)–(19d). In this context, Figures 3a and 3b can be interpreted as TPDs for particles located at x_0 in Ω_1 and Ω_2, respectively. Alternatively, when approximating $\Delta\mathbf{w}$ by a uniformly distributed random variable in the RWPM [see *Tompson et al.*, 1987], the uniform TPDs for particles located in Ω_1 and Ω_2 may be modified similarly, as was done by *Uffink* [1985]. For the more general one-dimensional problem with multiple interfaces, use of this modified uniform TPD together with small Δt can limit necessary image densities to those arising from a single interface.

Interpolation Technique

Discontinuities in the dispersion tensor can also be addressed through interpolation. This method, also discussed below in the context of random-walk particle tracking on a block-centered finite difference solution, smoothes the dispersion tensor in the vicinity of the interface to eliminate discontinuities and define the gradient term in the drift vector. For convergence to the true solution, this method requires convergence in time step as well as the spatial discretization associated the interpolation scheme. Below we evaluate interpolation and the reflection technique.

Comparison With Theory

We test the interpolation and reflection techniques in a closed one-dimensional constant-concentration system with reflecting boundaries on both ends and a partially reflecting interface located in the center such that the two equal-volume portions of the domain, Ω_1 and Ω_2, are delineated by a discrete contrast in dispersion coefficients [see *Semra et al.*, 1993]. When there is no drift in Ω_1 and Ω_2 ($\mathbf{A} = \mathbf{0}$), a correct technique will maintain a uniform particle number density on either side of the partially reflecting interface, i.e., $N_1/N_2 = 1$. Figure 4 shows results of a test of the alternative methods presented above using the RWPM for a one-dimensional system with reflecting boundaries at $x = -49$ and $x = 49$, $\Delta t = 0.005$, 588 particles, $D_1 = 5.0$ ($x < 0$), and D_2 ($x > 0$) prescribed such that the ratio D_1/D_2 ranges from 2.5 to 20.0. For this problem the alternative interpolation technique is applied by linearly interpolating D through a unit length across the interface at $x = 0$. The results for N_1/N_2 at an approximate steady state show that using no correction fails to maintain uniform number density. Interpolation and the method of *Uffink* [1985] correctly maintain a uniform number density.

To further test these methods, we compare results for a point source initial condition with the analytical solution given by (19a)–(19d) and illustrated in Figure 3a. A total of 100,000 particles were used in each simulation, wherein $x_0 = -5.0$, $D_1 = 5.0$, $D_2 = 0.25$, and $\Delta t = 0.005$. Figure 5 compares

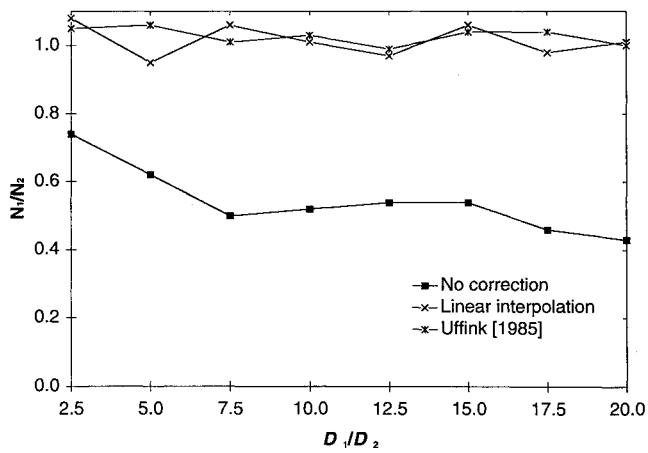

Figure 4. Comparison in ratios of particle numbers (N_1/N_2) on either side of discontinuity in D for different alternative techniques to conserve mass.

concentrations approximated at discrete spatial locations by the normalized number of particles contained in a unit length along the x axis with the analytical solution at time $t = 6.0$. The result labeled "no correction" clearly shows the error imposed by neglecting to reflect particles or interpolate. Interpolation and the method of *Uffink* [1985] compare well with the analytical solution.

Note the distinct differences between the two successful techniques. Uffink's technique simulates the exact TPD. Thus we consider this approach to converge strongly when the TPD is simulated using Wiener processes (strong convergence refers to the approach of a simulated particle path to the exact path $\mathbf{X}_p(t)$ [*Kloeden and Platen*, 1989]). Interpolation does not simulate the exact TPD but still balances mass.

Limitation of the Reflection Method

For many problems, *Uffink*'s [1985] reflection method may become computationally infeasible because of the need for multiple images (or reflections) around two- or three-dimensional discontinuities in the **D** field. A comparable situation arises with solutions to the flow problem through image well theory (e.g., no-flow boundaries intersecting at a right angle [*Ferris et al.*, 1962]). Although the number of images required for reasonably accurate solutions is finite (due to the normally small time steps used with the RWPM), this problem quickly becomes intractable for heterogeneous multidimensional systems. Interpolation, easily implemented in three dimensions, appears to provide a reasonable alternative to the method of images. Convergence, however, requires convergence in the spatial discretization associated with the interpolation as well as a simultaneous convergence with decreasing time-step size. In the following section, we address the application of velocity interpolation and a reflection principle to random walks on a block-centered finite difference flow solution and introduce a new algorithm based on a modified hybrid velocity interpolation scheme.

Interpolation Methods for Implementing The RWPM

Application of the RWPM requires knowledge of the groundwater velocity and velocity gradient at particle locations, which are typically determined by numerical solution of the relevant flow problem. As an example, consider the solution of a two-dimensional flow problem with no sources or sinks, as defined by

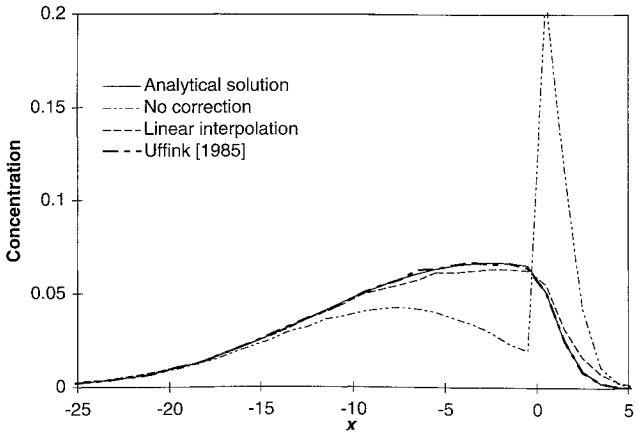

Figure 5. Comparison of concentrations from simulations using the different alternative techniques and the analytical solution given in (19a)–(19d) at $t = 6.0$ for $x_0 = -5.0$, $D_1 = 5.0$, and $D_2 = 0.25$. The method of *Uffink* [1985] produces results virtually identical to the analytical solution. The linear interpolation method yields a close approximation.

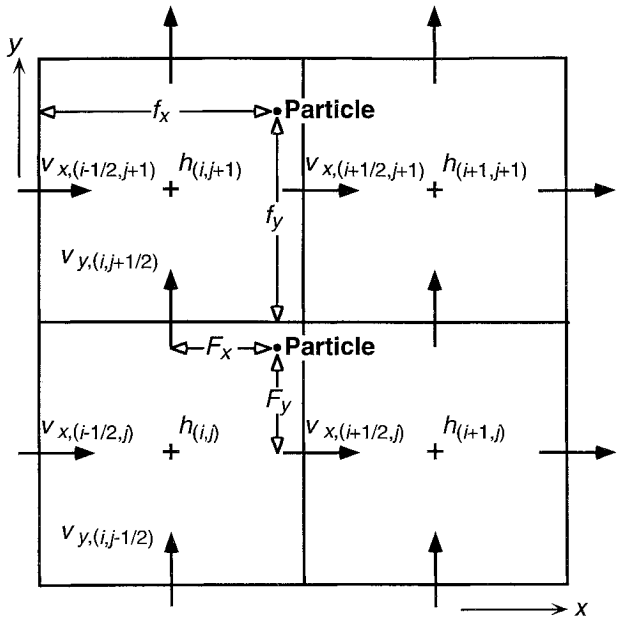

Figure 6. Velocity interpolation from a block-centered finite difference flow scheme.

$$\frac{\partial}{\partial x}\left(K_x \frac{\partial h}{\partial x}\right) + \frac{\partial}{\partial y}\left(K_y \frac{\partial h}{\partial y}\right) = 0 \tag{20}$$

where h is hydraulic head $[L]$ and K_x and K_y are the principal components of hydraulic conductivity in the x and y directions $[LT^{-1}]$. In terms of the RWPM, application of a block-centered finite difference scheme for the solution of (20) is particularly attractive because particles are easily located with respect to volumetric blocks in an orthogonal grid. Here, hydraulic conductivities are specified on a regular grid of nodes with coordinates $(i\Delta x, j\Delta y)$, and nodal values of the hydraulic head are determined from a finite difference approximation of (20):

$$\frac{1}{\Delta x}\left[\left(K_{x(i+1/2,j)}\frac{h_{(i+1,j)} - h_{(i,j)}}{\Delta x}\right) - \left(K_{x(i-1/2,j)}\frac{h_{(i,j)} - h_{(i-1,j)}}{\Delta x}\right)\right] + \frac{1}{\Delta y}\left[\left(K_{y(i,j+1/2)}\frac{h_{(i,j+1)} - h_{(i,j)}}{\Delta y}\right) - \left(K_{y(i,j-1/2)}\frac{h_{(i,j)} - h_{(i,j-1)}}{\Delta y}\right)\right] = 0 \tag{21}$$

where Δx and Δy are the constant nodal spacings $[L]$ (Figure 6). Intermediate (midnode) values of the conductivity are usually based on a harmonic average of the adjacent nodal values along a segment between two nodes.

Given a nodal solution for the heads, the most obvious way to estimate velocity components is to first compute midnode components along segments between two nodes, i.e.,

$$v_{x,(i+1/2,j)} = -\frac{1}{\Theta} K_{x(i+1/2,j)} \frac{h_{(i+1,j)} - h_{(i,j)}}{\Delta x} \tag{22}$$

Table 1. Velocity Interpolation Schemes

Interpolation Scheme	v_x	v_y
Linear*	$(1 - f_x)v_{x,(i-1/2,j)} + f_x v_{x,(i+1/2,j)}$	$(1 - f_y)v_{y,(i,j-1/2)} + f_y v_{y,(i,j+1/2)}$
Bilinear†	$(1 - F_y)[(1 - F_x)v_{x,(i,j)} + F_x v_{x,(i+1/2,j)}] + F_y[(1 - F_x)v_{x,(i,j+1/2)} + F_x v_{x,(i+1/2,j+1/2)}]$	$(1 - F_x)[(1 - F_y)v_{y,(i,j)} + F_y v_{y,(i,j+1/2)}] + F_x[(1 - F_y)v_{y,(i+1/2,j)} + F_y v_{y,(i+1/2,j+1/2)}]$
Block discrete	$\frac{1}{2}(v_{x,(i+1/2,j)} + v_{x,(i-1/2,j)})$	$\frac{1}{2}(v_{y,(i,j+1/2)} + v_{y,(i,j-1/2)})$

*Here, $f_x = (x - x_{i-1/2})/\Delta x$ and $f_y = (y - y_{j-1/2})/\Delta y$.
†Values apply over a block of dimension $\Delta x/2$ by $\Delta y/2$ centered on $(i + 1/4, j + 1/4)$; $F_x = 2(x - x_{i,j})/\Delta x$ and $F_y = 2(y - y_{i,j})/\Delta y$; x velocity terms are defined as $v_{1,(i,j)} = \frac{1}{2}(v_{1,(i+1/2,j)} + v_{1,(i-1/2,j)})$, $v_{1,(i+1/2,j+1/2)} = \frac{1}{2}(v_{1,(i+1/2,j+1)} + v_{1,(i+1/2,j)})$, and $v_{1,(i,j+1/2)} = \frac{1}{4}(v_{1,(i+1/2,j+1)} + v_{1,(i+1/2,j)} + v_{1,(i-1/2,j+1)} + v_{1,(i-1/2,j)})$.

As shown in Figure 6, this will yield normal components of velocity on the volumetric "block" surrounding node (i, j). However, information on all velocity components at one location is not provided in this way, nor is the velocity at any other point in the domain. Velocities at particle locations must be interpolated from these basic midnode values. Several approaches can be used to do this, as reviewed below.

Linear Interpolation

In the linear interpolation (LI) approach, one approximates velocity components linearly and independently within each block based on the available midnode values (Table 1). As such, there is no variation of v_x in the y direction, nor any variation of v_y in the x direction. Although derivatives of specific velocity components, as required to evaluate the divergence of the dispersion tensor, may not be fully defined, the interpolated velocity field within each block, $\mathbf{v}_{\mathrm{LI}}(\mathbf{x})$, satisfies the fluid mass balance $\nabla \cdot \mathbf{v} = 0$ exactly. The LI scheme may yield discontinuities in tangential velocities and therefore the velocity-dependent dispersion tensor, at block interfaces. Mass conservation therefore requires a reflection principle or alternative technique be applied at these interfaces. The LI scheme has been used in the context of advective particle tracking by *Pollock* [1988], *Goode* [1990], *Schafer-Perini and Wilson* [1991], and *Cordes and Kinzelbach* [1992].

Bilinear Interpolation

In the bilinear interpolation (BLI) approach, midnode velocity components surrounding a node are first averaged to provide estimates of velocity at the node (Table 1). In this way, both components are available at each location. The interpolated velocity may then be estimated in a bilinear fashion within cell volumes, or quarter segments of these volumes, as shown in Table 1 and Figure 6. Here, the interpolated velocity field, $\mathbf{v}_{\mathrm{BLI}}(\mathbf{x})$, does not satisfy fluid mass balance; however, it allows all first-order derivatives of velocity components to be estimated. An important advantage of BLI is that the dispersion tensor is continuous in this case; a reflection principle is therefore not required. *Konikow and Bredehoeft* [1978] applied BLI in a method of characteristics model, and *Goode* [1990] used it for advective particle tracking.

Block-Discrete Interpolation

In the block-discrete interpolation (BDI) approach, midnode velocity components are averaged to obtain values considered constant within specific finite difference blocks. *Tompson et al.* [1987] and *Tompson and Gelhar* [1990] focus on the cell volumes created by neighboring nodes to (1) average the midnode fluxes on each cell edge and obtain constant cell velocities, $\mathbf{v}_{\mathrm{BDI}}$, and (2) to form central difference approximations for estimating velocity gradients; these are also uniform within each grid block. This approach supports easy implementation of the RWPM because direct interpolation onto each particle is not required, but is otherwise very approximate. Nevertheless, if spatial variation of velocity is small with respect to the grid resolution, errors might still be acceptably small.

Hybrid Schemes

For purely advective particle tracking, the LI scheme is mass conservative and clearly an appropriate choice. However, for the dispersive component of the random walk, the LI scheme may be impractical because of the need for reflection corrections. This raises the possibility of applying LI for the advective component and BLI for velocities in the dispersive component. Below, we compare hybrid schemes that use bilinear interpolation to estimate velocities in the dispersion tensor, and either linear or block-discrete methods to approximate advective terms; we will refer to these hybrid schemes as BLI/LI and BLI/BDI, respectively. These hybrid schemes yield a continuous dispersion tensor, so a reflection principle is not required to satisfy mass balance at block interfaces.

Test Cases

Two problems are considered: (1) transport in highly permeable stratum bounded by low-permeability material in which transport occurs only by diffusion and (2) transport in two-dimensional heterogeneous porous media. The first problem assesses the relative accuracy, with respect to balancing mass at material contacts, of the three interpolation schemes and a reflection principle presented above by comparing results from numerical experiments with a known analytical solution. This problem serves as a surrogate for the general case, where due to the nature of the block-centered finite difference scheme, tangential velocities, and therefore the velocity-dependent dispersion tensor, are often discontinuous at block interfaces. Furthermore, this problem represents the "worst case scenario" of a discontinuous dispersion tensor that might be encountered in more general two- and three-dimensional simulations. The second problem demonstrates the potentially significant effects of neglecting discontinuities in the dispersion tensor in random-walk simulations of transport in complex heterogeneous porous media. In this case, results from hybrid interpolation schemes, BLI/LI and BLI/BDI, which locally balance mass by bilinearly interpolating velocities in the dispersion tensor, are compared with the BDI scheme of *Tompson et al.* [1987] and *Tompson and Gelhar* [1990], which tries to cor-

rect for these discontinuities by including approximations for gradient terms.

Solute Transport in a Stratified System

Problem description. The stratified saturated system shown in Figure 7 contains a thin horizontal high-permeability layer of thickness $2b$ and length 1.0 m. This layer is bounded by low-permeability porous layers considered to be of infinite thickness in the vertical. A conservative constituent is introduced at constant concentration, c_0, at the upstream end of the high-permeability layer during a time period t_p. As the constituent progresses along the high-permeability layer, diffusive transport between this layer and the adjacent low-permeability layers accentuates the overall dispersion of solutes in the system. Obtaining an accurate solution to this problem is highly dependent on a correct simulation of mass transfer across the interfaces between high- and low-permeability layers.

Initial and boundary conditions for the problem are specified as

$$c(x, y, 0) = 0 \tag{23a}$$

$$c(0, y, t) = c_0 \qquad 0 < t \leq t_p \qquad -b \leq y \leq +b \tag{23b}$$

$$c(0, y, t) = 0 \qquad \text{otherwise}$$

$$c(\infty, y, t) = 0 \tag{23c}$$

$$c(x, \pm\infty, t) = 0 \tag{23d}$$

For $t_p = 7$ days, these conditions represent a 7-day input of a conservative constituent at the upstream end of the high-permeability layer as was addressed in the laboratory study of *Sudicky et al.* [1985]. For this problem, the pore-scale longitudinal dispersivity has been shown to contribute little to the development of the solute plume, and neglecting it will introduce little error in predictions. For simplicity, the porosity was specified as a constant of 1.0 throughout the system. Superposition in time of the analytical solution presented by *Gillham et al.* [1984], which assumes that solute in the high-permeability layer is well mixed, is used to obtain an analytical solution to (23a)–(23d).

For the numerical experiments, the various interpolation schemes were incorporated into the SLIM1 random-walk code [*Tompson et al.*, 1987]. In all numerical simulations, the domain was discretized in a manner consistent with a velocity field computed by a block-centered finite difference flow model.

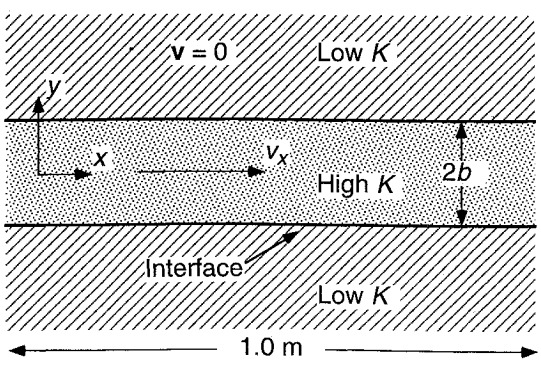

Figure 7. A stratified system with a thin high-permeability layer bounded by a low-permeability porous matrix.

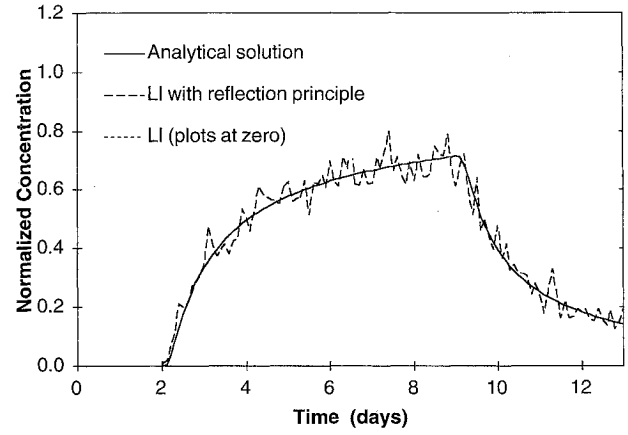

Figure 8. Comparison of analytical solution with solute breakthrough curve predicted using LI with and without a reflection principle ($\Delta y = 0.03$ m). There is no solute breakthrough for LI without a reflection principle. Simulations using $\Delta y = 0.01$ m and 0.006 m produce identical results for this test case.

The average concentration, $\bar{c}_H^s$, across the entire high-permeability layer at a point x may be discretely estimated from the particle mass contained within a narrow area centered at x of length Δx and width $2b$, divided by the area, $\Delta a = 2b\Delta x$. In terms of (2), with $\Theta = 1$, $\bar{c}_H^s$ can be expressed by

$$\bar{c}_H^s(x) = \left(\frac{1}{\Delta a}\right) \sum_p m_p \qquad \forall X_p \in \Delta a|_x \tag{24}$$

Transport in this stratified system may be modeled with the particle approach by releasing particles along the upstream edge of the high-permeability layer and allowing them to advect downstream and disperse into the adjacent low-permeability zones. To simulate the Dirichlet boundary condition at the upstream end of the system, the concentration, $\bar{c}_H^s$, in the leftmost column cells is maintained at a value of 1.0 for 7 days using a total of 5000 particles and properly maintained boundary conditions [*Tompson and Dougherty*, 1992], after which it is turned off.

Simulations were performed for three levels of discretization, $\Delta y = 0.03$ m, $\Delta y = 0.01$, and $\Delta y = 0.006$ corresponding to 1, 3, and 5 grid blocks, respectively, for the entire width of the high-permeability layer. Discretization in the x direction, used to calculate concentration, is specified as 0.001 m. The following parameter values were used in all simulations: $b = 0.015$ m, $D^m = 1.0454 \times 10^{-4}$ m^2/d, $\alpha_T = 0.01$ m, $v_1 = 0.5$ m/d, and $\Delta t = 0.001$ days.

Results and discussion. Simulations were performed for the LI scheme with and without a reflection principle. The results for $\bar{c}_H^s$ at $x = 1.0$ m are compared with the analytical solution in Figure 8. Predictions using LI with a reflection principle agree well with the analytical solution. Predictions using LI alone yield little or no solute breakthrough; mass in the high-permeability layer is lost to the low-permeability matrix. The discretization in the y direction does not affect results from either LI with a reflection principle or LI alone; hence the cases $\Delta y = 0.01$ m and $\Delta y = 0.006$ m are not shown.

The LI scheme without a reflection principle preserves discontinuities in velocity at material contacts and fails to address them. This is similar to the "no correction" case considered in

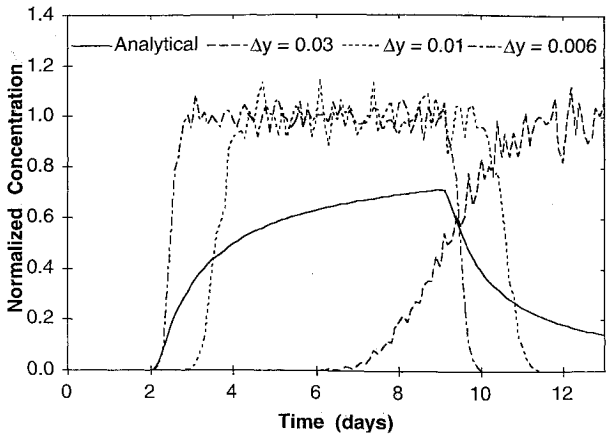

Figure 9. Comparison of analytical solution with solute breakthrough curves predicted using BDI.

the tests of the various reflection principles. Without special treatment of random walks at these contacts, mass flux from high- to low-dispersion layers is overestimated, and mass flux from low- to high-dispersion layers is underestimated.

Predictions using BDI are compared with predictions from the analytical solution in Figure 9. As expected, results from BDI compare poorly to the analytical solution because discontinuities in the velocity-dependent dispersion tensor are not addressed. The gradient terms in BDI seek to offset mass-conservation errors due to discontinuities. However, the magnitudes of these terms and the areas over which they apply change with discretization in the y direction, whereas the impulse in drift due to the discontinuity in the transverse dispersion is independent of this discretization.

Results from the BLI/LI and BLI/BDI hybrid schemes are compared with the analytical solution in Figure 10. Note that simulations using the BLI/LI and BLI/BDI hybrid schemes yield the same results for this test case. As expected, results indicate convergence of these schemes to the analytical solution as the grid is refined. As the grid becomes more coarse, breakthrough is shifted to later times; however, the main features of the breakthrough curves, in particular, peak concentrations, are maintained. The extent to which this BLI/LI and BLI/BDI can approximate discontinuous tangential velocities will depend on the resolution of the grid.

Ideally, one would also hope to test the BLI/LI hybrid scheme in cases with more complex heterogeneity in two- and three-dimensions. However, we know of no analytical solutions to represent a "ground truth" for such conditions. Furthermore, comparing with other numerical solutions would be circular. Nevertheless, we believe the above two-dimensional test is sufficient to conclude that the BLI/LI hybrid scheme is capable of producing reliable results, provided the discretization is adequately refined.

Transport in Heterogeneous Porous Media

Problem description. The transport of a conservative constituent in a heterogeneous system is considered here. This problem is of interest because the RWPM has been proposed [*Tompson et al.*, 1987] to verify stochastic transport theories [e.g., *Matheron and de Marsily*, 1980; *Gelhar and Axness*, 1983] and to investigate the effects of porous media heterogeneity on solute transport [*Tompson et al.*, 1994]. In these cases, random-walk model solutions are considered true representations of transport. Accuracy in these random-walk simulations is therefore critical.

The two-dimensional conductivity field illustrated in Figure 11 was generated on a grid with dimensions 85 ($\Delta z = 1$) in the vertical and 1400 ($\Delta x = 100$) in the horizontal using a Gaussian conditional simulation technique [*Fogg et al.*, 1991] with a spherical variogram model having vertical and horizontal variogram ranges of 10 and 400, respectively. For flow simulations, the numerical grid is refined in the x direction, so that $\Delta x = 10$, while still preserving the geometry of the simulated conductivity field. A steady state hydraulic-head distribution was simulated using the MODFLOW block-centered finite difference flow program [*McDonald and Harbaugh*, 1988]. No-flux boundary conditions are specified at $z = 0$ and $z = 85$. Constant-head boundary conditions at $x = 5$ and $x = 1395$ are specified as $h = 37$ and $h = 0$, respectively, for all z.

Transport is simulated for an instantaneous injection of a contaminant in a fully penetrating line source at location $x = 10$. Boundary conditions for transport simulations are specified as reflecting no-flux conditions at $z = 0$ and $z = 85$ and open boundaries at $x = 10$ and $x = 1390$. Initially, 50,000 particles are distributed uniformly over the vertical in the column of grid blocks from $x = 0$ to $x = 10$. These particles are allowed to advect and disperse into the domain over a single time step. After this time step, particles at locations $x < 10$ are eliminated in order to approximate an instantaneous injection of mass. The following parameter values are used in all simulations: $\Theta = 0.33$, $D^m = 1.1 \times 10^{-3}$, and $\alpha_L = \alpha_T = 0.03$.

Results and discussion. In this example, we use BDI, BLI, and the two hybrid schemes, BLI/LI and BLI/BDI, and compare results for mass-breakthrough curves and first and second spatial moments of the mass distribution [*Tompson et al.*, 1987]. Results for mass breakthrough at $x = 1390$ versus time from simulations using the various interpolation schemes are compared in Figure 12. Results for the first- and second-order moments are presented in Figures 13 and 14, respectively. For this problem, results from the three schemes that bilinearly interpolate velocities in the dispersion tensor are virtually identical, indicating little effect of change in advective-component interpolation method on predicted average transport behavior. In contrast, BDI model predictions differ considerably from the three BLI schemes, showing that average

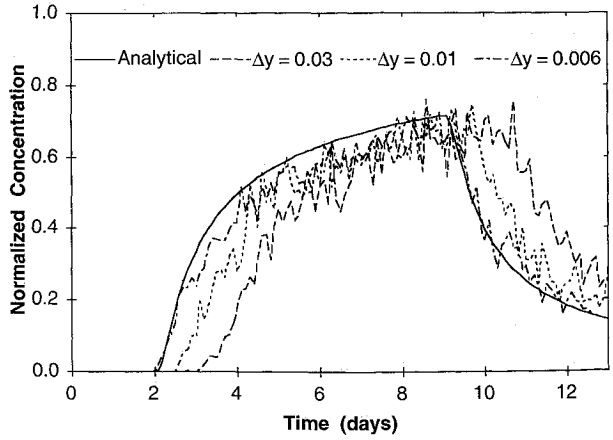

Figure 10. Comparison of analytical solution with solute breakthrough curves predicted using BLI/LI and BLI/BDI schemes. The BLI/LI and BLI/BDI schemes produce identical results for this test case.

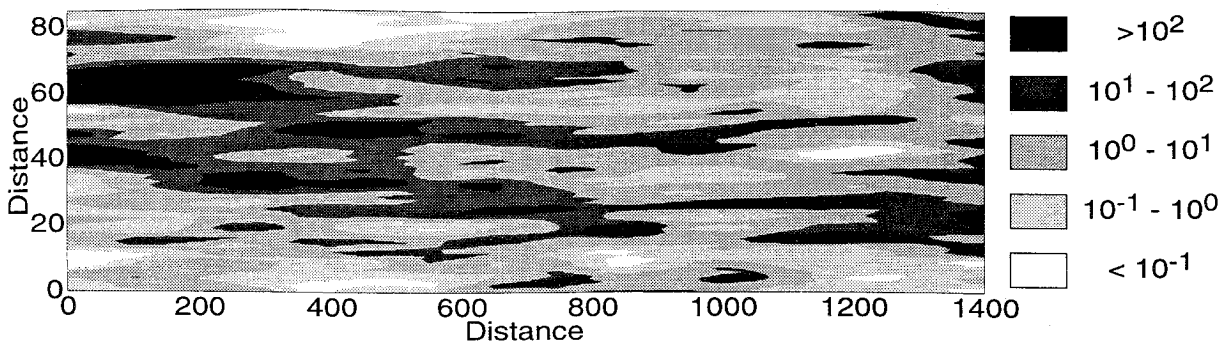

Figure 11. Gaussian conditional simulation of hydraulic-conductivity field with log K mean and standard deviation of 1.69×10^{-3} and 2.75×10^{-3}, respectively, and vertical and horizontal variogram ranges of 10 and 400, respectively (modified from *Fogg et al.* [1991]).

transport behavior predicted by the RWPM is sensitive to the way in which **D** is treated for this case.

Considerable effort has been devoted to accurate interpolation of velocities for the case of pure solute advection ($\mathbf{A} = \mathbf{v}$, $\mathbf{B} = \mathbf{0}$) [*Reddell and Sunada*, 1970; *Konikow and Bredehoeft*, 1978; *Pollock*, 1988; *Goode*, 1990; *Schafer-Perini and Wilson*, 1991; *Cordes and Kinzelbach*, 1992]. It is well known that by maintaining aquifer geometry at a given scale and refining the computational grid, in the limit, interpolation errors in advective components will vanish [*Goode*, 1990]. However, as demonstrated in the transport experiment in stratified media (Figures 8, 9, and 10), discontinuities in the dispersion tensor and the consequent mass-conservation errors will remain unless interpolation, reflection, or similar alternative method is applied. Agreement between schemes that bilinearly interpolate velocities in the dispersion tensor and disagreement between these schemes and BDI (Figures 12–14) suggest that when transport is dispersive ($\mathbf{D} \neq \mathbf{0}$), the choice of interpolation scheme for advective components has relatively little effect on overall transport compared to the choice of how one handles discontinuities in dispersion tensor.

Conclusions

In this paper we have reviewed conditions required for local mass conservation by the RWPM and discussed consequences of violating these conditions. A problem occurs in cases where interfaces separate materials with contrasting hydraulic properties; dispersivities, effective porosities, and velocities, and therefore the velocity-dependent dispersion tensor, may be discontinuous. We find that when the dispersion tensor is discontinuous, due to a discontinuous velocity field, mass flux can be conserved in the RWPM through the use of a carefully chosen interpolation scheme or a reflection principle. Similar methods may be applied when dispersivities or effective porosities are discontinuous.

A reflection principle based on the method of images yields a mass-conservative random walk near interfaces representing discontinuities in the dispersion tensor. However, application of this method to general three-dimensional problems in which multiple interfaces intersect appears problematic; numerous images (reflections) must be superimposed to obtain the transition probability density. Velocity interpolation provides a mass-conservative approximation that does not require superposition of multiple images. Velocity interpolation is easily implemented, and simulation results indicate convergence as the spatial and temporal discretizations are refined.

When a block-centered finite difference scheme is used to solve the flow equation, linear interpolation in the direction of the velocity component, although consistent with the governing flow equations, may yield discontinuities in tangential velocities, even when the effective porosity is continuous in space.

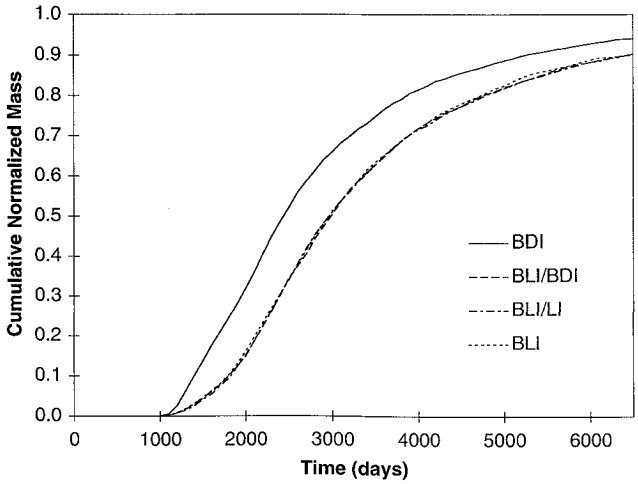

Figure 12. Comparison of solute breakthrough curves predicted using BDI, BLI/BDI, BLI/LI, and BLI.

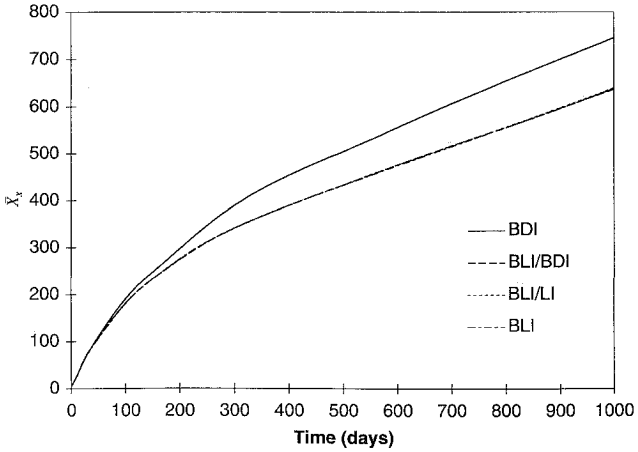

Figure 13. Comparison of first-order moments predicted using BDI, BLI/BDI, BLI/LI and BLI.

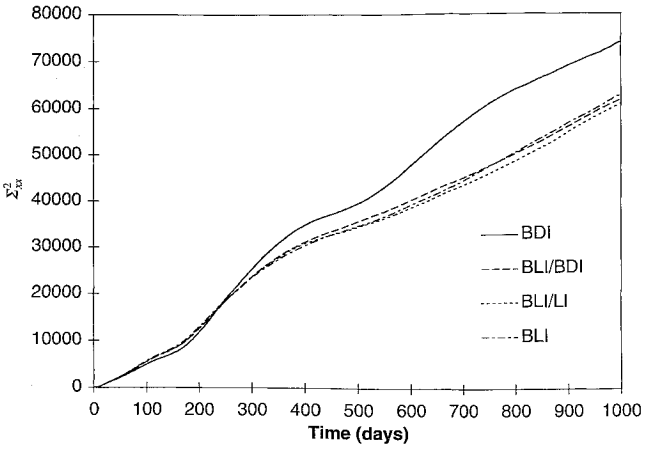

Figure 14. Comparison of second-order moments predicted using BDI, BLI/BDI, BLI/LI, and BLI.

These discontinuities are not a problem in advective particle-tracking models. However, with the RWPM, velocities tangent to an interface also contribute to the dispersive flux across that interface. Discontinuities in this flux violate local mass conservation. Bilinear (or trilinear) interpolation of velocities in the dispersion tensor or a reflection principle provide methods for conserving mass in these cases. The results presented herein show that, unless one of these methods (or a similar method) is applied, discontinuities in tangential velocities may lead to severe local mass-conservation errors in the random walk which can significantly affect transport predictions. Simulation results suggest local mass-conservation errors, due to incorrectly handling discontinuities in dispersive components of the random walk, outweigh mass-conservation errors due to inaccurate interpolation of advective components.

Last, we find that additional development of the theory behind the RWPM for the advection-dispersion equation with discontinuous coefficients is needed. While the interpolation approach has been applied with some success here, it appears that a more accurate, efficient method without the need for grid refinement might arise from such an effort.

Acknowledgments. This work was supported by grants from the U.S. Geological Survey, Monterey Water Resources Agency, U.S. EPA (R819658) Center for Ecological Health Research at U.C. Davis, and NIEHS Superfund Grant (ES-04699). Although the information in this document has been funded in part by the U.S. Environmental Protection Agency, it may not necessarily reflect the views of the agency, and no official endorsement should be inferred.

References

Ahlstrom, S. W., H. P. Foote, R. C. Arnett, C. R. Cole, and R. J. Serne, Multi-component mass transport model: Theory and numerical implementation, *Rep. BNWL-2127*, Battelle Pacific Northwest Lab., Richland, Washington, 1977.

Bagtzoglou, A. C., A. F. B. Tompson, and D. E. Dougherty, Projection functions for particle grid methods, *Numer. Methods Partial Differential Equations*, *8*, 325–340, 1992.

Bear, J., *Dynamics of Fluids in Porous Media*, Elsevier, New York, 1972.

Carslaw, H. S., and J. C. Jaeger, *Conduction of Heat in Solids*, pp. 363–365, Clarendon, Oxford, 1959.

Cordes, C., and W. Kinzelbach, Continuous groundwater velocity fields and path lines in linear, bilinear, and trilinear elements, *Water Resour. Res.*, *28*(11), 2903–2911, 1992.

Crank, J., *The Mathematics of Diffusion*, 2nd ed., pp. 162–164, Clarendon, Oxford, 1975.

Feller, W., *An Introduction to Probability Theory and Its Applications*, John Wiley, New York, 1957.

Ferris, J. G., D. B. Knowles, R. H. Brown, and R. W. Stallman, Theory of aquifer tests, *U.S. Geol. Surv. Water Supply Pap., 1536-E*, 1962.

Fogg, G. E., F. J. Lucia, and R. K. Senger, Stochastic simulation of interwell-scale heterogeneity for improved prediction of sweep efficiency in carbonate reservoirs, in *Reservoir Characterization II*, edited by L. W. Lake, H. B. Carroll Jr., and T. C. Wesson, pp. 355–381, Academic, San Diego, Calif., 1991.

Gardiner, C. W., *Handbook of Stochastic Methods for Physics Chemistry and the Natural Sciences*, Springer-Verlag, New York, 1990.

Gelhar, L. W., and C. W. Axness, Three-dimensional analysis of macrodispersion in aquifers, *Water Resour. Res.*, *19*(1), 161–180, 1983.

Gillham, R. W., E. A. Sudicky, J. A. Cherry, and E. O. Frind, An advection diffusion concept for solute transport in heterogeneous unconsolidated geologic deposits, *Water Resour. Res.*, *20*(3), 369–378, 1984.

Goode, D. J., Particle velocity interpolation in block-centered finite difference groundwater flow models, *Water Resour. Res.*, *26*(5), 925–940, 1990.

Kinzelbach, W., The random walk method in pollutant transport simulation, in *Groundwater Flow and Quality Modelling, NATO ASI Ser., Ser. C Math and Phys. Sci.*, vol. 224, edited by E. Custidio, A. Gurgui, and J. P. Lobo Ferreria, pp. 227–246, D. Reidel, Norwell, Mass., 1988.

Kloeden, P. E., and F. Platen, A survey of numerical methods for stochastic differential equations, *Stochastic Hydrol. Hydraul.*, *3*, 155–178, 1989.

Konikow, L. F., and J. D. Bredehoeft, Computer model of two-dimensional solute transport and dispersion in ground water, *Tech. Water Resour. Invest.*, book 7, chap. C2, U.S. Geol. Surv., Washington, D. C., 1978.

Matheron, G., and G. de Marsily, Is transport in porous media always diffusive? A counterexample, *Water Resour. Res.*, *16*(5), 901–917, 1980.

McDonald, M. G., and A. Harbaugh, A modular three-dimensional finite difference groundwater flow model, *Tech. Water Resour. Invest. 06-A1*, U.S. Geol. Surv., Washington, D. C., 1988.

Pollock, D. W., Semianalytical computation of path lines for finite difference models, *Groundwater*, *26*(6), 743–750, 1988.

Prickett, T. A., T. G. Naymik, and C. G. Longquist, A random walk solute transport model for selected groundwater quality evaluations, *Bull. Ill. State Water Surv.*, *65*, 1981.

Reddell, D. L., and D. K. Sunada, Numerical simulation of dispersion in groundwater aquifers, *Hydrol. Pap. 41*, Colo. State Univ., Fort Collins, 1970.

Risken, H., *The Fokker-Planck Equation*, Springer-Verlag, New York, 1989.

Schafer-Perini, A. L., and J. L. Wilson, Efficient and accurate front tracking for two-dimensional groundwater flow models, *Water Resour. Res.*, *27*(7), 1471–1485, 1991.

Semra, K., P. Ackerer, and R. Mosé, Three-dimensional groundwater quality modeling in heterogeneous media, in *Water Pollution II: Modeling, Measuring and Prediction*, edited by L. C. Wrobel and C. A. Brebbia, pp. 3–11, Comput. Mech., Billerica, Mass., 1993.

Sudicky, E. A., R. W. Gilham, and E. O. Frind, Experimental investigation of solute transport in stratified porous media, 1, The nonreactive case, *Water Resour. Res.*, *21*(7), 1035–1041, 1985.

Tompson, A. F. B., Numerical simulation of chemical migration in physically and chemically heterogeneous porous media, *Water Resour. Res.*, *29*(11), 3709–3726, 1993.

Tompson, A. F. B., and D. E. Dougherty, Particle-grid methods for reacting flows in porous media with application to Fisher's equation, *Appl. Math. Model.*, *16*, 374–383, 1992.

Tompson, A. F. B., and L. W. Gelhar, Numerical simulation of solute transport in three-dimensional randomly heterogeneous porous media, *Water Resour. Res.*, *26*(10), 2541–2562, 1990.

Tompson, A. F. B., E. G. Vomoris, and L. W. Gelhar, Numerical simulation of solute transport in randomly heterogeneous porous media: Motivation, model development, and application, *Rep. UCID-21281*, Lawrence Livermore Natl. Lab., Livermore, Calif., 1987.

Tompson, A. F. B., S. F. Ashby, R. D. Falgout, S. G. Smith, T. W. Fogwell, and G. A. Loosmore, Use of high performance computing

to examine the effectiveness of aquifer remediation, *Rep. UCRL-JC-115374*, Lawrence Livermore Natl. Lab., Livermore, Calif., 1994.

Uffink, G. J. M., A random walk method for the simulation of macrodispersion in a stratified aquifer, Relation of Groundwater Quality and Quantity, *IAHS Publ. 146*, 103–114, 1985.

Uffink, G. J. M., Modeling of solute transport with the random walk method, in *Groundwater Flow and Quality Modelling, NATO ASI Ser., Ser. C Math and Phys. Sci.*, vol. 224, edited by E. Custidio, A. Gurgui, and J. P. Lobo Ferreria, pp. 247–265, D. Reidel, Norwell, Mass., 1988.

G. E. Fogg and E. M. LaBolle, Hydrologic Science, Veihmeyer Hall, University of California, Davis, Davis, CA 95616-8628. (e-mail: gefogg@ucdavis.edu)

A. F. B. Thompson, Lawrence Livermore National Laboratory, Livermore, CA 94550.

(Received June 22, 1995; revised November 13, 1995; accepted November 16, 1995.)